

Experimental determination of the boundary condition for diffuse photons in a homogeneous turbid medium

David L. Everitt, Tuo Zhu, H.-M. Zhu, and X. D. Zhu*

Department of Physics, University of California at Davis, One Shields Avenue, Davis, California 95616-8677

Received August 12, 1999; revised manuscript received February 29, 2000; accepted March 13, 2000

We present a simple experimental method that permits an empirical determination of the effective boundary condition and the extrapolated end point for the diffuse photon density in a homogeneous turbid medium.

© 2000 Optical Society of America [S0740-3232(00)00307-0]

OCIS codes: 170.7050, 170.6960, 290.7050.

In recent years interest has been growing in understanding light transport through a turbid (i.e., highly scattering) medium and in imaging objects in such a medium based on the distribution of a diffusely scattered light in the medium.^{1,2} In the interior of a turbid medium, the light transport is described by the diffusion approximation of the radiative transport theory.^{3,4} Within the diffusion approximation, diffusely scattered photons perform independent random walks characterized by a transport mean free path ℓ_{tr} . As a result, the photon number density, or diffuse photon density, satisfies a diffusion equation that includes absorption.

Near the surface of a turbid medium within a few transport mean free paths, the diffusion equation is no longer satisfied by the diffuse photon density. It is known that the diffuse photon density in the interior would vanish asymptotically at a distance beyond the physical boundary. Such a distance is called the extrapolated end point ϵ .³ In cases in which the refractive indices of the turbid medium and the adjoining scattering-free medium are matched, ϵ is found theoretically to equal $0.71\ell_{tr}$.³⁻⁵ Knowing ϵ , one can then write down an effective boundary condition for the diffuse photon density in a turbid medium. The distribution of the diffuse photon density has been used for imaging absorptive objects in turbid media. To the best of our knowledge, the theoretical prediction of $\epsilon = 0.71\ell_{tr}$ has not been confirmed experimentally.

In this paper we present a simple experimental method that enables us to measure the extrapolated end point ϵ . Using this method, we find that for a number of commonly used turbid media, ϵ consists of two terms: One term varies linearly with the scattering mean free path ℓ_s and roughly equals $0.71\ell_{tr}$ with $\ell_{tr} = \ell_s/(1-g)$; the other term, not known before this study, is independent of ℓ_s . Here $g \equiv \langle \cos \theta \rangle_{av}$ is the anisotropy factor of scattering of the medium, with θ being the scattering angle. The first term can be used to measure the transport mean free path ℓ_{tr} and the anisotropy factor g . The second term is large enough that one should take it into consid-

eration when using diffuse photon density distributions for tomographic imaging.

Our experimental method measures the diffuse photon density distribution in a turbid medium along a straight path perpendicular to a boundary surface. The turbid medium in our study is of a rectangular geometry and is contained in a long rectangular fused silica cell (100B-QS, from Hellma Cells, N.J.). The inside of the cell has the following dimensions: length (L) 10.0 mm \times width (W) 9.45 mm \times height (H) 50 mm. One pair of opposing side walls are made of black fused silica so that the light entering these walls will be completely absorbed. The other pair of side walls are transparent. Through one of the latter we uniformly illuminate one side of the rectangular turbid medium with a continuous-wave He-Ne laser at 633 nm and measure with an imaging optics the near-field distribution of the diffuse photon flux that emerges from the opposite side. The top view of the experimental sketch is shown in Fig. 1. We choose the center of the rectangular turbid medium as the origin, and the y axis is along the direction of transmittance. The surface at $y = -L/2$ is illuminated.

The diffuse photon density in the interior of a turbid medium $\Phi(x, y, z)$ is governed by the diffusion equation and satisfies an appropriate boundary condition. In the rectangular geometry, $\Phi(x, y, z)$ can be generally written as

$$\Phi(x, y, z) = \sum_{n=0,1,2} \chi_n(y, z) \cos \left[\frac{(2n+1)\pi x}{W+2\epsilon} \right]. \quad (1)$$

We assume that $\Phi(x, y, z)$ vanishes at an extrapolated end point ϵ outside the boundary surfaces that are not illuminated, namely, $\Phi(x, y = L/2 + \epsilon, z) = 0$ and $\Phi(x = \pm L/2 \pm \epsilon, y, z) = 0$. For a rectangular turbid medium that is long along the z direction (i.e., $H \gg L$, and $H \gg W$), it is easily shown that $|\chi_n(y, z)| \gg |\chi_{n+1}(y, z)|$. As a result, one needs only to consider the first two terms,

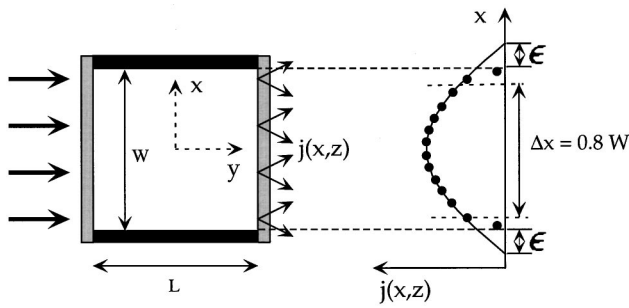


Fig. 1. Top view of the experimental arrangement. A tall rectangular fused silica cell with width $W = 9.45$ mm, length $L = 10.0$ mm, and height $H = 50$ mm is filled with a turbid medium. Two cell walls are black. One surface of the medium at $y = -L/2$ is illuminated uniformly. The diffuse photon flux $j(x, z)$ (solid circles) emerging from the opposite surface at $y = L/2$ is detected with an imaging optics and a CCD detector (not shown). $j(x, z)$ from $x = -0.4W$ to $x = 0.4W$ or $\Delta x = 0.8W$ is fitted to theory to yield the extrapolated end point ϵ .

$$\Phi(x, y, z) \approx \chi_0(y, z) \cos[\pi\chi/(W + 2\epsilon)] + \chi_1(y, z) \cos[3\pi\chi/(W + 2\epsilon)],$$

with the first term dominating. Since the diffuse photon flux that emerges from the surface at $y = L/2$ is proportional to $\Phi(x, y, z)$ at a small distance (of the order of the transport mean free path) inside the medium,³⁻⁶ it should have the following form:

$$j(x, z)|_{y=L/2} = a_0(z) \cos[\pi x/(W + 2\epsilon)] + a_1(z) \cos[3\pi x/(W + 2\epsilon)]. \quad (2)$$

Experimentally we measure $j(x, z)|_{y=L/2}$ at $z = 0$ by imaging the surface of the turbid medium at $y = L/2$ onto a 16-bit CCD detector. We deduce ϵ by fitting the measured $j(x, z = 0)|_{y=L/2}$ to Eq. (2). In our case $a_1(z)/a_0(z) \sim 0.002$. Because $\Phi(x, y, z)$ satisfies the diffusion equation only in the interior of the medium (at least one transport mean free path away from the boundary surface²), we use only the flux data taken from $x = -0.4W$ to $x = 0.4W$ to obtain the asymptotic behavior of $\Phi(x, y, z)$ beyond the boundary.

We perform the experiment on a number of commonly used turbid media. The media include (a) Intralipid emulsion (Kabi Pharmacia, Clayton, N.C.), (b) TiO_2 particles (Sigma Coatings, San Diego, Calif.) in glycerol, and (c) aqueous suspensions of monodispersed polystyrene latex spheres (Duke Scientific, Palo Alto, Calif.) of diameters $2.01 \pm 0.022 \mu\text{m}$, $2.88 \pm 0.03 \mu\text{m}$, $0.497 \pm 0.006 \mu\text{m}$, and $0.370 \pm 0.004 \mu\text{m}$. At the optical wavelength of 633 nm we can neglect the residual absorption in these media. Our Monte Carlo simulation shows that the residual absorption in Intralipid emulsion at 633 nm causes less than 1% change in the extrapolation end points. For all three types of turbid media investigated, the flux data fit extremely well to Eq. (2). The width W of the rectangular turbid medium along the x direction covers 220 pixels. The pixel density is high enough that the finite spatial resolution of our CCD detector has no discernible effect on the determination of ϵ . For each medium we separately measure the extrapolated end point ϵ and the scattering mean free path ℓ_s . To measure ℓ_s we

pass a He-Ne laser beam through a wedge-shaped gap (formed between two fused quartz plates) that is filled with the turbid medium in question. The thickness d of the gap varies from less than $1 \mu\text{m}$ to $100 \mu\text{m}$ or $600 \mu\text{m}$. We measure the intensity $I(d)$ of the unscattered He-Ne laser beam. $I(d)$ fits perfectly to a single exponential function $I(d) = I_0 \exp(-d/\ell_s)$ over three orders of magnitude. From the fit we deduce ℓ_s .

In Fig. 2 we plot the measured ϵ versus ℓ_s . For each medium we change the concentration such that ℓ_s varies by at least one order of magnitude. We find that ϵ indeed varies linearly with ℓ_s for all the media studied, with ϵ/W being as large as 0.16. The linear dependence is not surprising, as it is predicted theoretically.^{3,4} In fact, it validates our present experimental approach. What is surprising is that ϵ approaches a nonzero constant or an intercept δ when ℓ_s approaches zero. For all three types of turbid media, the intercepts are roughly the same and are equal to 0.35 mm. This means that $\delta/W \sim 4\%$. The results can be summarized by expressing ϵ as a linear function of ℓ_s with an intercept δ :

$$\epsilon = \gamma \ell_s + \delta. \quad (3)$$

By comparing with other independently determined anisotropy factors g for monodispersed polystyrene spheres in water and Intralipid emulsion, we find that the first term in Eq. (3) equals the theoretical prediction of $0.71\ell_s/(1 - g)$ such that

$$\epsilon = 0.71\ell_s/(1 - g) + \delta. \quad (4)$$

To show this, we deduced the anisotropy factor g using the slope $\gamma = d\epsilon/d\ell_s$ and Eq. (4). The deduced g factors are tabulated in Table 1. For monodispersed polystyrene spheres in water, we have also calculated the g factors using the Mie scattering theory, and the results are also displayed in Table 1.⁷ Our experimental values agree with

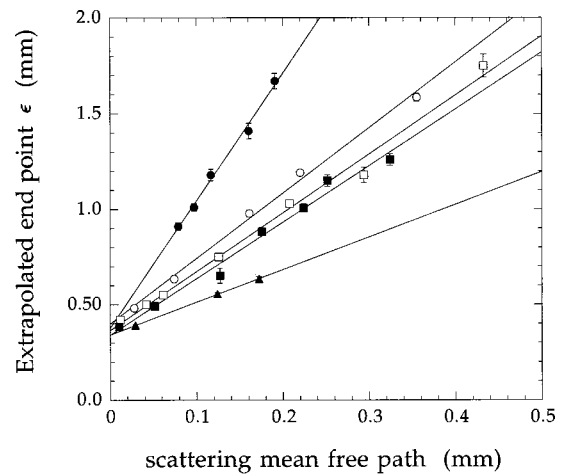


Fig. 2. Measured extrapolated end point ϵ versus the scattering mean free path ℓ_s for aqueous solution of latex spheres with a diameter of $2.01 \mu\text{m}$ (solid circles), aqueous solution of latex spheres with a diameter of $2.88 \mu\text{m}$ (open circles), aqueous solution of latex spheres with a diameter of $0.37 \mu\text{m}$ (solid triangles), TiO_2 particles in glycerol (open squares), and Intralipid emulsion (solid squares).

Table 1. Anisotropy Factors g for Various Turbid Media

Turbid Medium	Theoretical	Other	Measurement ^a
	Values	Measurements	
Intralipid emulsion		0.75–0.88 ^d	0.77
TiO ₂ in glycerol			0.77
2.01- μm latex sphere	0.90 ^b		0.90
2.88- μm latex sphere	0.82 ^b		0.81
0.497- μm latex sphere	0.82 ^b		0.79
0.370- μm latex sphere	0.73 ^b		0.61
Monte Carlo system	0.90 ^c		0.90
Monte Carlo system	0.75 ^c		0.75
Monte Carlo system	0.50 ^c		0.51

^a Obtained by fitting $d\epsilon/d\ell_s$ to $0.71/(1-g)$ in this work.

^b Calculated from Mie theory for aqueous solution of polystyrene latex spheres at an optical wavelength of 632.8 nm.

^c Prescribed in our Monte Carlo simulations.

^d Reference 8.

the theoretical values within 5% for three of the four particle diameters tested. For Intralipid emulsion, our result of $g = 0.77$ agrees with the values reported in the literature within 10%.⁸ The good agreements show that our present experimental procedure is reliable as a general method to determine the transport mean free path ℓ_{tr} and the anisotropy factor g . For TiO₂ in glycerol, the TiO₂ particles are polydispersed. We do not have information as to the size and shape distribution of these TiO₂ particles. As a result we are not able to compute g factors for the purpose of comparison. There is no independent measurement of g factors of such TiO₂ mixture in glycerol.

The intercept δ in Eq. (4) is unexpected theoretically. We should point out that the observed δ is not the result of reflection or index mismatch at the interface between an interrogated turbid medium and the fused silica wall.⁵ In the case of TiO₂ in glycerol, the refractive index for glycerol ($n_{\text{glycerol}} = 1.474$) matches very well with that for fused silica ($n_{\text{silica}} = 1.457$), and yet the intercept δ is found the same as the intercepts for monodispersed polystyrene spheres in water ($n_{\text{water}} = 1.33$) and for Intralipid emulsion. At this point, we do not understand the origin of such an ℓ_s -independent term in the extrapolated end point. For applications such as tomographic imaging of turbid media based on diffuse photon measurements, such a term is significantly large that one has to take it into consideration in the boundary condition. Because $\delta/W \sim 4\%$, neglecting such a term would result in a few percent error in the computed diffuse photon density, and such an error is easily amplified in the image reconstruction process into sizable artifacts in the image field. The amplification effect arises from the high sensitivity of a diffuse photon tomographic imaging to errors

in the measurement and in the model that includes the presumed boundary condition.

To further validate our experimental procedure and to examine whether the ℓ_s -independent term in the extrapolated end point could be accounted for if the light scattering in the near boundary region is treated exactly, we performed a Monte Carlo simulation that emulates the experiment. The turbid medium in the simulation has the same rectangular geometry and the same scattering properties as the ones studied in our experiment. In the simulation we follow the trajectories of 10^9 photons that are uniformly incident onto the surface of a rectangular turbid medium at $y = -L/2$. The photons subsequently traverse through the medium by means of their respective sequences of random walks. In each random-walking step along a trajectory, a photon is assigned a randomly chosen jump length and is then scattered into a randomly chosen scattering direction. The jump lengths follow a Poisson distribution with a prescribed scattering mean free path ℓ_s . The scattering angles are selected on the basis of the Henyey–Greenstein approximation⁹ to the Mie scattering theory with a prescribed anisotropy factor g_{prescr} . We performed simulations for three values of g_{prescr} : 0.5, 0.75, and 0.90. For each anisotropy factor, we vary ℓ_s in a range comparable with the ranges for the real turbid media studied. When a photon is found outside the medium after a jump, it is presumed to propagate freely in the direction of the jump. At the opposite surface at $y = L/2$ with a width W along the x direction, we assign the emerging photons to 200 bins according to their exit locations over the width W of the medium along the x axis. The bin number of 200 is chosen to be comparable with that of the CCD pixels (220) used in our experiment. We fit the diffuse photon flux distribution in the central 160 bins to Eq. (2) to deduce the extrapolated end point ϵ . The simulation data fit very well to Eq. (2).

We find that the extrapolated end point ϵ_{MC} obtained from the Monte Carlo simulations also varies linearly with ℓ_s and has a small intercept δ_{MC} with $\delta_{\text{MC}}/W \sim 0.003$. From the slopes $d\epsilon_{\text{MC}}/d\ell_s$ and assuming that $d\epsilon_{\text{MC}}/d\ell_s = 0.71\ell_s/(1-g_{\text{MC}})$, we obtain the anisotropy factors $g_{\text{MC}} = 0.51, 0.75, \text{ and } 0.90$. These values agree almost perfectly with the respective g_{prescr} values of 0.5, 0.75, and 0.90. This further confirms our experimental procedure as a simple and reliable method for obtaining the transport mean free path and the anisotropy factor. Our Monte Carlo algorithm also provides an independent check on our experimental methodology and on the subsequent analysis based on the diffusion model. The fitted and the prescribed values of the g factors are listed in Table 1 for comparison.

It is noteworthy that the intercept δ_{MC} is also present in our Monte Carlo simulation. However, it is small as $\delta_{\text{MC}}/W \sim 0.003$. If we scaled the Monte Carlo simulation result to the size of the real turbid media with $W = 9.45$ mm, the value of δ_{MC} would be roughly 0.03 mm, at least a factor of 10 smaller than the measured intercepts of 0.35 mm. This means that the large ℓ_s -independent term in the extrapolated end point as observed for real turbid media cannot be accounted for by treating the fate of diffuse photons near the surface region more precisely.

ACKNOWLEDGMENTS

We thank Gus Hart for assistance in implementing the Monte Carlo algorithm. The work is supported by the U.S. Department of Energy Center of Excellence for Laser Application in Medicine under grant DEFG0398ER62576.

*Address correspondence to X. D. Zhu at xdzhu@physics.ucdavis.edu.

REFERENCES

1. "Diffuse photons in turbid media," B. Tromberg, A. Yodh, E. Sevick, and D. Pines, eds. (feature issue), *Appl. Opt.* **36**, 9–231 (1997); "Diffuse photons in turbid media," B. Tromberg, A. Yodh, E. Sevick, and D. Pines, eds., *J. Opt. Soc. Am. A* **14**, 136–342 (1997).
2. A. Yodh and B. Chance, "Spectroscopy and imaging with diffusing light," *Phys. Today* **48**, 34–40 (1995).
3. K. M. Case and P. F. Zweifel, *Linear Transport Theory* (Addison-Wesley, London, 1967).
4. A. Ishimaru, *Wave Propagation and Scattering in Random Media* (Academic, London, 1978), Vol. 1, pp. 175–180.
5. R. Aronson, "Boundary conditions for diffusion of light," *J. Opt. Soc. Am. A* **12**, 2532–2539 (1995), and references therein.
6. R. C. Haskell, L. O. Svaasand, T.-T. Tsay, T.-C. Feng, M. S. McAdams, and B. J. Tromberg, "Boundary conditions for the diffusion equation in radiative transfer," *J. Opt. Soc. Am. A* **11**, 2727–2741 (1994).
7. C. F. Bohren and D. R. Huffman, *Absorption and Scattering of Light by Small Particles* (Wiley, New York, 1983).
8. H. J. van Staveren, C. J. M. Moes, J. van Marle, S. A. Prahl, and J. C. van Gemert, "Light scattering in Intralipid-10% in the wavelength range of 400–1100 nm," *Appl. Opt.* **30**, 4507–4514 (1991).
9. L. G. Henyey and J. L. Greenstein, "Diffuse radiation in the galaxy," *Astrophys. J.* **93**, 70–83 (1941).